Monolithic integration of erbium-doped amplifiers with silicon-on-insulator waveguides

Laura Agazzi,[1*] Jonathan D. B. Bradley,[1] Meindert Dijkstra,[1] Feridun Ay,[1] Gunther Roelkens,[2] Roel Baets,[2] Kerstin Wörhoff,[1] and Markus Pollnau[1]

[1]*Integrated Optical Microsystems Group, MESA+ Institute for Nanotechnology, University of Twente, P.O. Box 217, 7500 AE Enschede, Netherlands*
[2]*Photonics Research Group, Department of Information Technology (INTEC), Ghent University, Sint-Pietersnieuwstraat 41, 9000 Gent, Belgium*
*l.agazzi@ewi.utwente.nl

Abstract: Monolithic integration of Al_2O_3:Er^{3+} amplifier technology with passive silicon-on-insulator waveguides is demonstrated. A signal enhancement of >7 dB at 1533 nm wavelength is obtained. The straightforward wafer-scale fabrication process, which includes reactive co-sputtering and subsequent reactive ion etching, allows for parallel integration of multiple amplifier and laser sections with silicon or other photonic circuits on a chip.

OCIS codes: (140.4480) Optical amplifiers; (130.3130) Integrated optics materials.

References and links

1. M. Lipson, "Guiding, modulating, and emitting light on silicon – challenges and opportunities," J. Lightwave Technol. **23**(12), 4222–4238 (2005).
2. W. Bogaerts, R. Baets, P. Dumon, V. Wiaux, S. Beckx, D. Taillaert, B. Luyssaert, J. Van Campenhout, P. Bienstman, and D. Van Thourhout, "Nanophotonic waveguides in silicon-on-insulator fabricated with CMOS technology," J. Lightwave Technol. **23**(1), 401–412 (2005).
3. M. Gnan, S. Thoms, D. S. Macintyre, R. M. De La Rue, and M. Sorel, "Fabrication of low-loss photonic wires in silicon-on-insulator using hydrogen silsesquioxane electron-beam resist," Electron. Lett. **44**(2), 115–116 (2008).
4. G. L. Bona, R. Germann, and B. J. Offrein, "SiON high-refractive-index waveguide and planar lightwave circuits," IBM J. Res. Develop. **47**(2), 239–249 (2003).
5. K. Wörhoff, C. G. H. Roeloffzen, R. M. de Ridder, A. Driessen, and P. V. Lambeck, "Design and application of compact and highly tolerant polarization-independent waveguides," J. Lightwave Technol. **25**(5), 1276–1283 (2007).
6. F. Morichetti, A. Melloni, M. Martinelli, R. G. Heideman, A. Leinse, D. H. Geuzebroek, and A. Borreman, "Box-shaped dielectric waveguides: A new concept in integrated optics?" J. Lightwave Technol. **25**(9), 2579–2589 (2007).
7. Q. Xu, B. Schmidt, S. Pradhan, and M. Lipson, "Micrometre-scale silicon electro-optic modulator," Nature **435**(7040), 325–327 (2005).
8. G. Masini, L. Colace, G. Assanto, H. C. Luan, K. Wada, and L. C. Kimerling, "High responsivity near infrared Ge photodetectors integrated on Si," Electron. Lett. **35**(17), 1467–1468 (1999).
9. A. W. Fang, H. Park, Y. H. Kuo, R. Jones, O. Cohen, D. Liang, O. Raday, M. N. Sysak, M. J. Paniccia, and J. E. Bowers, "Hybrid silicon evanescent devices," Mater. Today **10**(1–2), 28–35 (2007).
10. G. Roelkens, J. Van Campenhout, J. Brouckaert, D. Van Thourhout, R. Baets, P. Rojo Romeo, P. Regreny, A. Kazmierczak, C. Seassal, X. Letartre, G. Hollinger, J. M. Fedeli, L. Di Cioccio, and C. Lagehe-Blanchard, "III-V/Si photonics by die-to-wafer bonding," Mater. Today **10**(7–8), 36–43 (2007).
11. K. Wörhoff, J. D. B. Bradley, F. Ay, D. Geskus, T. P. Blauwendraat, and M. Pollnau, "Reliable low-cost fabrication of low-loss Al_2O_3:Er^{3+} waveguides with 5.4-dB optical gain," IEEE J. Quantum Electron. **45**(5), 454–461 (2009).
12. C. A. Barrios, and M. Lipson, "Electrically driven silicon resonant light emitting device based on slot-waveguide," Opt. Express **13**(25), 10092–10101 (2005).
13. D. R. Zimmerman, and L. H. Spiekman, "Amplifiers for the masses: EDFA, EDWA, and SOA amplets for metro and access applications," J. Lightwave Technol. **22**(1), 63–70 (2004).
14. J. D. B. Bradley, M. Costa e Silva, M. Gay, L. Bramerie, A. Driessen, K. Wörhoff, J. C. Simon, and M. Pollnau, "170 Gbit/s transmission in an erbium-doped waveguide amplifier on silicon," Opt. Express **17**(24), 22201–22208 (2009).
15. M. Nakazawa, T. Yamamoto, and K. R. Tamura, "1.28 Tbit/s-70 Km OTDM transmission using third- and fourth-order simultaneous dispersion compensation with a phase modulation," Electron. Lett. **36**(24), 2027–2029 (2000).

16. L. H. Spiekman, "Semiconductor optical amplifiers," in *Optical Fiber Telecommunications Volume IVA*, I. P. Kaminow and T. Li, eds. (Academic Press, 2002), pp. 699–731.
17. S. Blaize, L. Bastard, C. Cassagnètes, and J. E. Broquin, "Multiwavelengths DFB waveguide laser arrays in Yb-Er codoped phosphate glass substrate," IEEE Photon. Technol. Lett. **15**(4), 516–518 (2003).
18. E. H. Bernhardi, H. A. G. M. van Wolferen, L. Agazzi, M. R. H. Khan, C. G. H. Roeloffzen, K. Wörhoff, M. Pollnau, and R. M. de Ridder, "Ultra-narrow-linewidth, single-frequency distributed feedback waveguide laser in $Al_2O_3:Er^{3+}$ on silicon," Opt. Lett. **35**(14), 2394–2396 (2010).
19. Frankfurt Laser Company, *http://www.frlaserco.com/*
20. J. Seufert, M. Fischer, M. Legge, J. Koeth, R. Werner, M. Kamp, and A. Forchel, "DFB laser diodes in the wavelength range from 760 nm to 2.5 µm," Spectrochem. Acta Part A **60**(14), 3243–3247 (2004).
21. G. Roelkens, P. Dumon, W. Bogaerts, D. Van Thourhout, and R. Baets, "Efficient silicon-on-insulator fiber coupler fabricated using 248 nm deep UV lithography," IEEE Photon. Technol. Lett. **17**(12), 2613–2615 (2005).
22. G. N. van den Hoven, R. J. I. M. Koper, A. Polman, C. van Dam, K. W. M. van Uffelen, and M. K. Smit, "Net optical gain at 1.53 µm in Er-doped Al_2O_3 waveguides on silicon," Appl. Phys. Lett. **68**(14), 1886–1888 (1996).
23. J. D. B. Bradley, F. Ay, K. Wörhoff, and M. Pollnau, "Fabrication of low-loss channel waveguides in Al_2O_3 and Y_2O_3 layers by inductively coupled plasma reactive ion etching," Appl. Phys. B **89**(2–3), 311–318 (2007).
24. J. D. B. Bradley, R. Stoffer, A. Bakker, L. Agazzi, F. Ay, K. Wörhoff, and M. Pollnau, "Integrated $Al_2O_3:Er^{3+}$ zero-loss optical amplifier and power splitter with 40 nm bandwidth," IEEE Photon. Technol. Lett. **22**(5), 278–280 (2010).
25. J. D. B. Bradley, L. Agazzi, D. Geskus, F. Ay, K. Wörhoff, and M. Pollnau, "Gain bandwidth of 80 nm and 2 dB/cm peak gain in $Al_2O_3:Er^{3+}$ optical amplifiers on silicon," J. Opt. Soc. Am. B **27**(2), 187–196 (2010).
26. J. D. B. Bradley, R. Stoffer, L. Agazzi, F. Ay, K. Wörhoff, and M. Pollnau, "Integrated $Al_2O_3:Er^{3+}$ ring lasers on silicon with wide wavelength selectivity," Opt. Lett. **35**(1), 73–75 (2010).
27. *ePIXfab, the silicon photonic platform. http://www.epixfab.eu/*
28. X. Phoeni, *http://www.phoenixbv.com/*
29. O. V. Ivanova, R. Stoffer, L. Kauppinen, and M. Hammer, "Variational effective index method for 3D vectorial scattering problems in photonics: TE polarization," in *Progress In Electromagnetics Research Symposium,* (The Electromagnetics Academy, Moscow, 2009), pp. 1038–1042.
30. M. Hammer, "Quadridirectional eigenmode expansion scheme for 2-D modeling of wave propagation in integrated optics," Opt. Commun. **235**(4–6), 285–303 (2004).
31. OlympIOs Integrated Optics Software, *http://www.c2v.nl/software/*
32. L. Agazzi, K. Wörhoff, A. Kahn, H. Scheife, G. Huber, and M. Pollnau are preparing a manuscript to be called "Microscopic treatment of energy-transfer upconversion and additional quenching mechanisms in rare-earth-ion-doped materials".
33. S. Selvaraja, D. Vermeulen, M. Schaekers, E. Sleeckx, W. Bogaerts, G. Roelkens, P. Dumon, D. Van Thourhout, and R. Baets, "Highly efficient grating coupler between optical fiber and silicon photonic circuit," in *Conference on Lasers and Electro-Optics*, Technical Digest (CD) (Optical Society of America, Washington, DC 2009), paper CTuC6. *http://www.opticsinfobase.org/abstract.cfm?uri=CLEO-2009-CTuC6*

1. Introduction

Within the last decade silicon-on-insulator (SOI) technology has rapidly developed into a well-established photonics platform [1] for a wide range of passive integrated optics applications operating in the near-infrared wavelength range. Although the typical propagation losses of silicon waveguides (0.9-3 dB/cm) [1–3] are significantly higher than the values of <0.1 dB/cm achieved in Si-compatible dielectric technology [4–6], the high refractive index contrast of silicon waveguides allows for shorter devices and densely integrated optical circuits. Low-loss bends with radii down to 5 µm are realized in silicon photonics. Furthermore, CMOS compatibility and an existing processing infrastructure add to the attractiveness of this technology. Besides passive functions, integrated modulation schemes [7] and light detection [8] are addressed. However, one fundamental drawback of Si photonics, the lack of efficient light generation because of the indirect bandgap in Si, remains.

Light generation on silicon chips can be achieved by integration of III-V semiconductor optical amplifiers (SOA) or rare-earth-ion (RE) doped dielectric thin films. Both approaches yield their specific advantages and drawbacks [8]. While the former requires hybrid integration schemes such as die-to-wafer bonding [9,10], the latter allows for direct wafer-scale deposition onto silicon substrates [11]. On the other hand, electrical pumping of SOAs provides a clear advantage over optical pumping of RE ions. Thus far, electrically pumped RE-doped dielectrics in a slotted Si-waveguide configuration have been proposed [12], but an experimental verification is still missing. In addition, SOAs deliver a gain per unit length of a few hundred dB/cm [13], while their dielectric counterparts typically provide only a few dB/cm [11,13].

Nevertheless, for specific applications RE-doped dielectrics are superior to III-V semiconductors. In an Er-doped waveguide amplifier on a Si wafer, amplification at bit rates up to 170 Gbit/s was recently demonstrated without noise penalty or patterning effects [14]. And there is the prospect for higher bit rates, as in Er-doped fibers high-speed amplification of an optical time division multiplexed and polarization multiplexed signal has reached 1.28 Tbit/s [15]. In contrast, when operating SOAs in a saturated or quasi-saturated gain regime, eye closure occurs, because their carrier lifetime of typically 100 ps causes transient gain suppression and recovery depending on bit rate and sequence [16]. Furthermore, laser linewidths of free-running single-longitudinal-mode distributed-feedback (DFB) lasers as narrow as 1.7 kHz have been demonstrated in RE-doped materials [17,18], while the typical linewidth of commercially available III-V DFB lasers ranges from 1 to 10 MHz [19,20]. Last but not least, operation of SOAs is more strongly influenced by temperature than their dielectric counterparts [13]. With increasing temperature the gain spectrum shifts significantly in wavelength, which can result in mode hopping. With RE-doped dielectrics instead, temperature stabilization can often be avoided altogether.

In this paper, we present a new approach and first experimental results on wafer-scale monolithic integration of active Er-doped dielectric waveguide technology with passive Si photonics. The integration concept and technological choices are discussed and our specific device design, fabrication aspects, and amplifier measurements are presented.

2. Integration concept and design

2.1 Integration concept of active and passive technologies

The integration concept is depicted in Fig. 1. In the same plane of an SOI chip, silicon photonic functions like passive circuitry and pump/signal multiplexing (MUX) and demultiplexing (DEMUX) sections (black) are integrated with Er-doped active functions (red), such as lossless fiber-chip couplers, high-speed amplifiers, and narrow-linewidth lasers. The active and passive functions are connected through silicon photonic wires (blue), which are inversely tapered into the Er-doped dielectric channel waveguides to ensure low-loss coupling of pump and signal light. Besides enabling high coupling efficiency, this type of coupler offers a large optical bandwidth [21], which is essential for exploiting active functions operating over a correspondingly large gain bandwidth. The active sections can be fabricated in multiple copies at any position on the chip by a simple two-step parallel process: deposition of the active thin film and subsequent reactive ion etching of the channel waveguides. As long as sufficient pump power is available, pumping of multiple amplifier and laser sections can be achieved by coupling a single diode laser, splitting its power on-chip, and launching it into the Er-doped sections.

For implementing this concept, requirements on the active technology are high-quality waveguide layers, sufficiently high gain over a broad wavelength range, a reliable, Si-compatible wafer-scale deposition process, and a high refractive index n of the active waveguide material. The latter enables the realization of compact integrated gain devices and small waveguide cross-sections, requiring lower pump power to achieve the same pump intensity, hence allowing a single diode laser to pump a larger number of active device sections on the chip.

We have chosen Er-doped amorphous aluminum oxide (a-Al$_2$O$_3$) as the gain material. Its broad transparency spectrum and high RE-ion solubility make Al$_2$O$_3$ an excellent host for active ions [22]. Reactive co-sputtering allows for straightforward deposition on different substrates. As-deposited planar waveguides and dry-etched channel waveguides with losses as low as 0.1 dB/cm and 0.2 dB/cm, respectively, are reliably fabricated [11,23]. Furthermore, the refractive index of a-Al$_2$O$_3$ ($n = 1.65$ at $\lambda = 1.55$ μm) is high compared to other typical dielectric hosts, such as silica ($n = 1.45$) or phosphate glass ($n = 1.55$). Low-loss bends with radii below 500 μm were demonstrated in a compact, 0.5×1.5 μm^2 waveguide cross-section [24]. For Er concentrations of 1-2 $\times$ 10^{20} cm^{-3}, amplification a with net peak gain of 2.0 dB/cm at $\lambda = 1533$ nm and a gain bandwidth of 80 nm ($\lambda = 1500$-1580 nm) was achieved

[25], resulting in the realization of a range of on-chip integrated active devices, such as a high-speed amplifier operated at 170 GBit/s [14], a zero-loss optical power splitter [24], a wavelength-selective ring laser operating almost across the entire telecom C-band [26], as well as an ultra-narrow-linewidth (1.7 kHz) DFB laser [18]. Therefore, this technology fulfills all of the basic requirements for integration on a SOI platform.
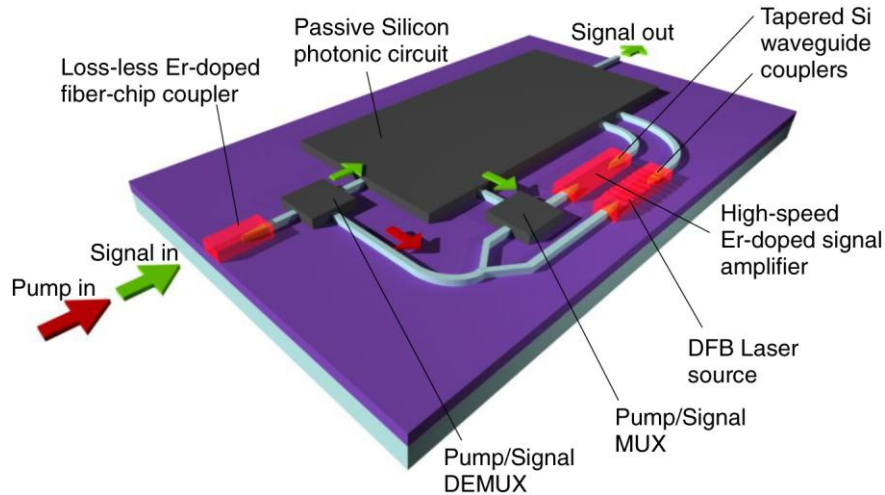

Fig. 1. Schematic of a SOI on-chip optical circuit including monolithically integrated Al_2O_3:Er^{3+} waveguide amplifiers and lasers (red sections)

2.2. Concept implementation and design

The SOI platform uses chips of size 13.5×29 mm^2 produced in a multi-user run of the epixfab CMOS line [27], with a 2-μm-thick silicon oxide (SiO$_2$) buffer and a 220-nm thick single-crystalline SOI layer. For single-mode waveguide operation, the channel width is set to 450 nm. Typical propagation losses of 2.4 dB/cm are achieved [2]. The Si channel waveguides are designed for TE-polarized light propagation.

The parameters of the active Al_2O_3:Er^{3+} sections were adapted to these boundary conditions. A minimum thickness of 1 μm was calculated for the Al_2O_3 film in order to avoid coupling of the propagating mode through the 2-μm-thick SiO$_2$ buffer layer to the silicon substrate. The channel width and etch depth of the Al_2O_3 film were determined to be 2.5 μm and 270 nm, respectively, for single-mode operation of randomly polarized light, 97% overlap between the pump ($\lambda = 1480$ nm) and signal ($\lambda = 1533$ nm) mode profiles, and a confinement of these modes within the active region of >80%. The coupling efficiency for launching light from a standard single-mode fiber into the Al_2O_3 channel waveguide was calculated with PhoeniX FieldDesigner software [28] to be 20%. Although fiber-chip coupling can be significantly improved [5], it was not the focus of the present study. An optimal Er concentration of 2.70×10^{20} cm^{-3} was calculated, taking into account the maximum amplifier length which was limited by the available chip length of 13.5 mm, and the available launched pump power of up to 50 mW.

Inverted Si tapers were designed in order to expand the Si waveguide mode and efficiently couple light from the Si to the Al_2O_3:Er^{3+} waveguide. The minimum feature size that can be realized in the Si etching process is 100 nm. For the given SOI and Al_2O_3 geometries the taper design was optimized by varying the taper length and shape in calculations based on a 3-dimensional fully vectorial eigenmode expansion method. A coupling loss as low as 0.5 dB induced by the Si-Al_2O_3:Er^{3+} coupler was calculated for the optimum design in which the width of the 450-nm Si channels is decreased linearly to 100 nm over a 400-μm-long tapering section. A summary of all geometrical parameters of the active / passive test devices is provided in Fig. 2.

In the final device design two Al_2O_3:Er^{3+} waveguides with a combined total length of 9.5 mm were linked through a 4-mm-long Si waveguide with inverted tapers at both ends, creating a 13.5-mm-long Al_2O_3:Er^{3+}-Si-Al_2O_3:Er^{3+} structure. Straight Al_2O_3:Er^{3+} channel waveguides with the same design parameters, but without Si features, were added as a reference device.
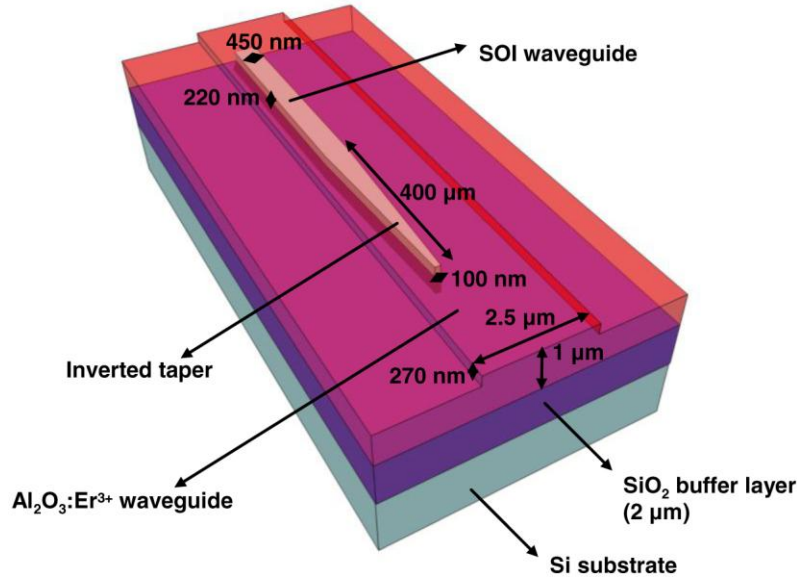

Fig. 2. Schematic of the designed geometries of the SOI and Al_2O_3:Er^{3+} waveguides as well as the adiabatically inverted taper structure for efficient light coupling

3. Experimental results

The process flow for the fabrication of integrated Si-Al_2O_3:Er^{3+} structures is depicted in Fig. 3. The Si waveguides were fabricated using state-of-the-art CMOS fabrication tools in a 200-mm CMOS pilot line. 193-nm-deep UV lithography was applied to define the 450-nm-wide channel waveguides and inverted taper structures (Fig. 3a). A SEM image of the 100-nm-wide tip of the inverted taper is shown in Fig. 4a. An Al_2O_3:Er^{3+} layer of 1030 nm thickness with an Er concentration of $(2.70 \pm 0.18) \times 10^{20}$ cm^{-3} was deposited onto the SOI structures by reactive co-sputtering (Fig. 3b). SEM images of cross-sections of the overgrown Si channels are depicted in Figs. 4b and 4c. The cross-sectional views are taken along the Si inverted taper showing the silicon channel at two different widths. Al_2O_3:Er^{3+} ridge-type channel waveguides were then defined by standard lithography and reactive ion etching (Fig. 3c). The alignment accuracy of the Al_2O_3:Er^{3+} channel waveguides on top of the Si photonic wire was within $\pm$ 0.5 μm which is the tolerance of our lithographic equipment. The resulting channels were 2.5 μm wide and the etch depth was 270 nm. Finally, the end-facets of the active/passive chips were diced to enable fiber butt-coupling to the Al_2O_3:Er^{3+} waveguides.

Losses in the Si-Al_2O_3:Er^{3+} couplers were measured by comparing the transmission of 1533-nm light in Al_2O_3:Er^{3+}-Si-Al_2O_3:Er^{3+} structures and straight Al_2O_3:Er^{3+} channel waveguides. Losses of ~2.5 dB per coupler were determined.
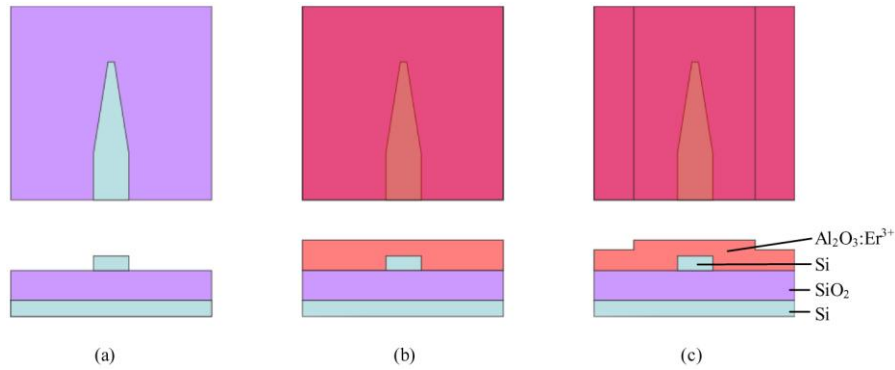
Fig. 3. Process flow for integration of Al_2O_3:Er^{3+} and Si waveguides (top view and cross-sectional view). (a) SOI waveguide; (b) deposition of the Al_2O_3:Er^{3+} layer; (c) structuring of the Al_2O_3:Er^{3+} layer
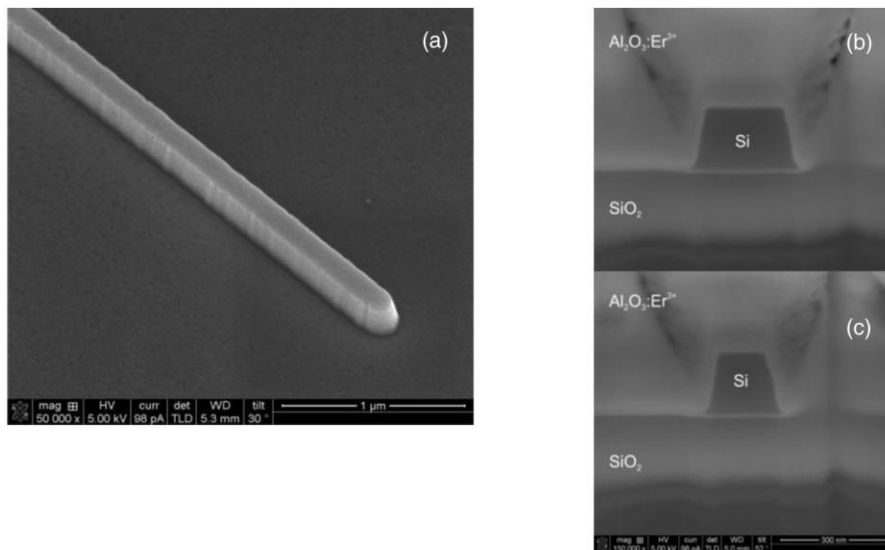

Fig. 4. (a) Scanning electron microscope (SEM) picture of an inversely tapered Si waveguide end before deposition of Al_2O_3:Er^{3+}; (b and c) SEM cross-sectional pictures of the tapered Si waveguide with decreasing horizontal size, covered by the Al_2O_3:Er^{3+} overlay

The signal enhancement was measured in the 13.5-mm-long Al_2O_3:Er^{3+}-Si-Al_2O_3:Er^{3+} structure. Since the Si waveguides were designed to operate only in TE polarization, we restricted the signal enhancement measurements to this polarization, although the Al_2O_3:Er^{3+} sections would enable operation at both, TE and TM polarization [25]. 1480-nm pump light from a pig-tailed laser diode and modulated signal light from a tunable laser source operated at different wavelengths relevant for the C-band were combined by a wavelength-division-multiplexing (WDM) fiber coupler and simultaneously launched into the device. The coupled signal power was varied between ~1 to 100 µW to provide information on the small-signal-gain limit. A second WDM coupler placed at the output of the chip and detection with standard lock-in amplification were employed to discriminate the outcoupled signal light from residual pump light and amplified spontaneous emission. By insertion loss measurements the pump coupling efficiency was determined to be 19%, in good agreement with the calculated value of 20%. The maximum launched pump power was 53 mW. The signal enhancement S was calculated from the equation

$$S = 10 \cdot \log_{10}\left[I_p / I_u \right], \tag{1}$$

where I_p and I_u are the transmitted signal intensities in the pumped and unpumped case, respectively. In Fig. 5a the signal enhancement in the Al_2O_3:Er^{3+}-Si-Al_2O_3:Er^{3+} structure is shown as a function of launched pump power for 1-µW signals at wavelengths of 1525 nm and 1565 nm, corresponding to the edges of the C-band, and 1533 nm, the gain peak of Al_2O_3:Er^{3+}. An enhancement of 7.2 dB was measured for the peak wavelength of 1533 nm at a launched pump power of 53 mW. To our knowledge, this is the first demonstration of wafer-scale monolithic integration of Er-doped dielectric amplifiers with Si channel waveguides. The signal enhancement measurement for different 1533-nm signal powers is shown in Fig. 5b. The small-signal-gain regime is evident for the lower signal power values, whereas saturation effects start to show up when signals of 100 µW are launched.
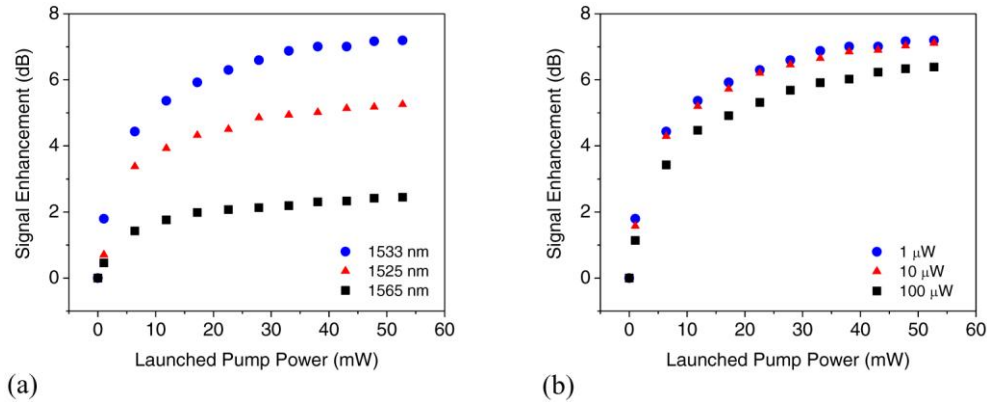

Fig. 5. Signal enhancement in a 13.5-mm-long Al_2O_3:Er^{3+}-Si-Al_2O_3:Er^{3+} structure as a function of launched pump power (a) for three different C-band wavelengths and (b) for varying signal input power at the peak wavelength of 1533 nm

4. Discussion

As mentioned above, losses of ~2.5 dB in the Si-Al_2O_3:Er^{3+} couplers were measured. The increase compared to the simulated coupler losses of 0.5 dB was explained by the mode leaking from the Al_2O_3:Er^{3+} channel into residual silicon structures on both sides of the coupling section, which were in too close proximity to the inverted tapers and could not be removed from the demonstrator chips. In case of perfect horizontal alignment of the Al_2O_3:Er^{3+} with the Si waveguides, the residual Si structures are spaced by 1.25 µm from the edge of the Al_2O_3:Er^{3+} channel waveguide. The interaction length between the optical mode and the residual Si structures is on the order of 100 µm. Light coupling into the residual Si structures was calculated by a variational effective index method in combination with a quadridirectional eigenmode propagation solver [29,30]. For horizontal Al_2O_3 channel misalignment of 0 µm, 0.25 µm, and 0.5 µm, losses into the Si of 70 dB/cm, 105 dB/cm, and 190 dB/cm, respectively, were calculated. The same alignment tolerance was applied to calculate the impact on the coupling loss in the taper coupler in the absence of residual Si structures by the beam propagation method [31]. A misalignment of 0.5 µm results in only 0.2 dB additional loss. We conclude that the additional 2-dB loss in the coupler section is mainly due to the residual Si structures, which are a matter of design modification to be addressed in future fabrication. Although owing to the additional loss induced by the residual Si structures no net gain could be demonstrated with the present Al_2O_3:Er^{3+}-SOI devices, one can compare the measured signal enhancement to that in Al_2O_3:Er^{3+} amplifier devices deposited on thermally oxidized silicon wafers [11]. In the latter, net gain was demonstrated for Er concentrations of 0.5-4 $\times$ 10^{20} cm^{-3} [25]. From Eq. (4) in [25] and Eq. (1), the signal enhancement S (dB) over the total amplifier length L can be calculated as

$$S(\lambda) = \left[\gamma(\lambda) + \alpha_{\text{Total}}(\lambda) \right] \cdot L, \tag{2}$$

where $\gamma(\lambda)$ is the internal net gain (dB/cm) and $\alpha_{\text{Total}}(\lambda)$ is the total propagation loss coefficient (sum of propagation and Er-absorption losses, in dB/cm). To determine the ideal internal net gain $\gamma(\lambda)$ of a standard Al_2O_3:Er^{3+} waveguide amplifier with the experimental length $L = 9.5$ mm and Er concentration of $(2.70 \pm 0.18) \times 10^{20}$ cm^{-3} of the Al_2O_3:Er^{3+} section of the current device, the rate-equation model described in [32] was applied. At the maximum launched pump power of 50 mW the result is an internal net gain of 1.96 ± 0.07 dB/cm at the 1533-nm signal wavelength. For the same wavelength a total propagation loss coefficient $\alpha_{\text{Total}}(\lambda)$ of 6.06 ± 0.44 dB/cm is extrapolated from the loss measurements reported in [25]. Consequently, from Eq. (2) a signal enhancement of 7.62 ± 0.48 dB is calculated, in good agreement with the 7.2 dB measured in the Al_2O_3:Er^{3+}-Si-Al_2O_3:Er^{3+} structure. Based on this comparison we conclude that Al_2O_3:Er^{3+} amplifiers integrated with SOI waveguides can achieve the same internal net gain as demonstrated in our standard Al_2O_3:Er^{3+} channel waveguides.

Light coupling from a single-mode fiber to the chip can be largely improved with a horizontally and vertically inverted Al_2O_3:Er^{3+} taper. When setting the minimum width at the taper tip to 800 nm (because of fabrication constrains) and the etch depth to 270 nm (as for the presented amplifiers), the optimized channel cross-section at the fiber-chip interface has dimensions of 800×325 nm^2 and a fiber-chip coupling efficiency of 76.9% (1.15 dB loss) is calculated at $\lambda = 1533$ nm. This value is a significant improvement over the 19% reported above for the non-optimized device and is even higher than the 69.5% coupling efficiency currently achieved in SOI grating couplers [33]. Moreover, the wavelength dependence of taper-based couplers is due mainly to the material dispersion. The coupling efficiency of our Al_2O_3:Er^{3+} couplers exhibits a variation of only 1% from the 1480-nm pump wavelength up to 1565 nm, while the strong wavelength dependence of SOI grating couplers results in a drop of the coupling efficiency from 69.5% to 31.6% and 8.9%, respectively, at these two wavelengths [33]. The small wavelength dependence of the inverted taper couplers largely adds to their attractiveness. However, their implementation requires a SiO_2 buffer thickness larger than 2 μm to avoid light coupling into the Si substrate. A SiO_2 thickness of >4.6 μm was calculated to keep these additional losses below 0.01 dB/cm. Finally, coupling both pump and signal light into the chip through this taper, as proposed in Fig. 1, would supply enough gain to entirely compensate the fiber-chip coupling loss for the signal light, thereby creating a loss-less fiber-chip coupler or even a pre-amplifier.

A next-generation device design could be based on a spiral shape that enables amplifiers with lengths up to tens of centimeters, while occupying a footprint area as small as 6×6 mm^2 [25]. The amplification which can be realized with such a layout was calculated based on an Er^{3+} concentration of 2.70×10^{20} cm^{-3}. For a 1480-nm pump power of 260 mW available at the pigtailed diode output, resulting in a launched pump power of ~200 mW for the 76.9% fiber-to-chip coupling efficiency, a gain of 42 dB over a 25-cm-long amplifier section is predicted. Such a high gain, in combination with the small footprint and the potential for wafer-scale processing with low fabrication complexity, makes this amplifier approach highly desirable for future silicon photonic devices.

4. Conclusions

A novel approach for the integration of Al_2O_3:Er^{3+} gain structures with silicon photonics has been developed and implemented. A signal enhancement of 7.2 dB at 1533 nm has been demonstrated in an Al_2O_3:Er^{3+}-Si-Al_2O_3:Er^{3+} structure. The performance is comparable to the results obtained with traditional Al_2O_3:Er^{3+} amplifier devices, indicating that internal net gain can be achieved in these integrated structures. Optimization of silicon taper losses, fiber-to-chip coupling efficiency, as well as total amplifier length and footprint can result in a net gain of more than 40 dB on a silicon photonic chip for an incident pump power of 260 mW. Al_2O_3:Er^{3+} is a promising candidate for monolithic wafer-scale integration of active functions

onto a passive SOI photonic platform. This type of integration yields a large potential for the realization of complex optical functionalities in combination with active devices such as high-speed amplifiers and arrays of narrow-linewidth DFB lasers.